

NOTE

Spectroscopic Determination of Oxidation and Coordination States of Mo Cations in the Reduced Mo/Al₂O₃ Catalyst

CO and NO can be selectively adsorbed as probe molecules on the catalytically active coordinatively unsaturated sites (cus) of reduced Mo/Al₂O₃ (1–3). More recently, the coadsorption of CO–NO has proved to be a useful probe for the characterization of active centers on the W/Al₂O₃ system (4). Although various oxidation states on the reduced molybdena-based catalysts have been claimed to be present, contradictions still exist between infrared results published by various researchers (1–3, 5–7).

Recently, the surface structure of the Mo/Al₂O₃ system in oxidic state has been well characterized by Raman spectroscopy (8). Dehydration was found to change the molecular structure of surface molybdenum oxide species under ambient conditions. Thus, in comparison with the IR results which are generally obtained after dehydration, the present Raman data were recorded *in situ* under dehydrated conditions. This work focuses on the structural changes of the 10% Mo/Al₂O₃ catalyst as a function of reduction temperature. The IR spectroscopy of adsorbed CO and coadsorbed CO–NO in combination with *in situ* Raman spectroscopy were used to elucidate the oxidation and coordination states of cus Mo cations under dehydrated conditions.

The support was γ -Al₂O₃ with S_{BET} of 200 m² g⁻¹. A 10 wt% Mo/Al₂O₃ sample was prepared by incipient wetness impregnation from an aqueous solution of ammonium heptamolybdate, followed by drying at 393 K and calcining at 723 K for 10 h.

The *in situ* Raman spectra were obtained at room temperature using a Jobin–Ivon Ramanor U-1000 spectrometer. The sample wafer was put into a quartz cell and was treated in a flow of dry O₂ (30 ml/min) at 700 K for 1 h. After dehydration, the gas stream was switched to H₂ at room temperature and the sample was reduced at the desired temperature for 0.5 h. The 488.0-nm line of an Argon-ion laser (Spectra Physics) was used as the excitation source. The laser power at the source was 200 mW.

The infrared spectra were recorded on a Perkin–Elmer 580B double-beam spectrometer with a resolution of 2.3 cm⁻¹. The cell used and the adsorption apparatus have been described in an earlier paper (4). The self-supporting

13-mm-diameter wafer was treated in a flow of H₂ (30 ml/min) at the desired temperature for 2 h, then evacuated at 673 K for 2 h (10⁻⁵ Torr). Subsequently, the sample was cooled and exposed to CO ($p = 30$ Torr) at room temperature for 1 h to obtain IR spectra of adsorbed CO. Then, NO was allowed to contact the sample for another 2 h to obtain the IR spectra of coadsorbed CO–NO.

The infrared spectra of CO and CO–NO adsorptions on 10% Mo/Al₂O₃ reduced at different temperatures are presented in Fig. 1. No adsorption bands on the oxidic sample were detected. Reduction at 473 K also did not produce any adsorption sites for CO or NO. After reduction at 573 K, CO adsorption results in a broad weak band at 2183 cm⁻¹. With the increase of reduction temperature up to 773 K, the frequency of adsorbed CO shifts downward to 2174 cm⁻¹.

When CO is coadsorbed with NO, the spectra in Figs. 1c–1e show a weak band at 2200–2190 cm⁻¹ which is most possibly due to CO adsorbed on cus Mo⁵⁺ sites (5, 7). A sharper CO band at ~2134 cm⁻¹ was observed, together with two intense NO bands at 1812 and 1708 cm⁻¹ due to adsorbed dinitrosyl species or an NO dimer (1, 3). Except for the weak ~2200-cm⁻¹ band, the intensities of the CO band at ~2134 cm⁻¹ and NO bands at 1812 and 1708 cm⁻¹ all increase considerably with increasing reduction temperature, indicating an increase in the total amount of the cus Mo cations. Additionally, the intensity ratio of the symmetric (1812 cm⁻¹) and anti-symmetric (1708 cm⁻¹) stretching bands also increases, which is due to the increase in NO coverage resulting from increasing extent of reduction (10).

Figure 2 shows the IR spectra of preadsorbed CO on 10% Mo/Al₂O₃ ($R_T = 673$ K) as a function of NO coadsorption time. On coadsorption with NO, simultaneously with the decrease of the preadsorbed CO band at 2178 cm⁻¹, a new CO band grows up at 2134 cm⁻¹, while strong twin NO bands appear at ~1809 and ~1704 cm⁻¹. The drastic shift of the CO band from 2178 to 2134 cm⁻¹ when coadsorbed with NO indicates that an electron transfer to the antibonding π^* orbital of CO is taking place (11). Evacuation at room temperature readily eliminates the CO band at 2134 cm⁻¹ and two NO bands at the higher

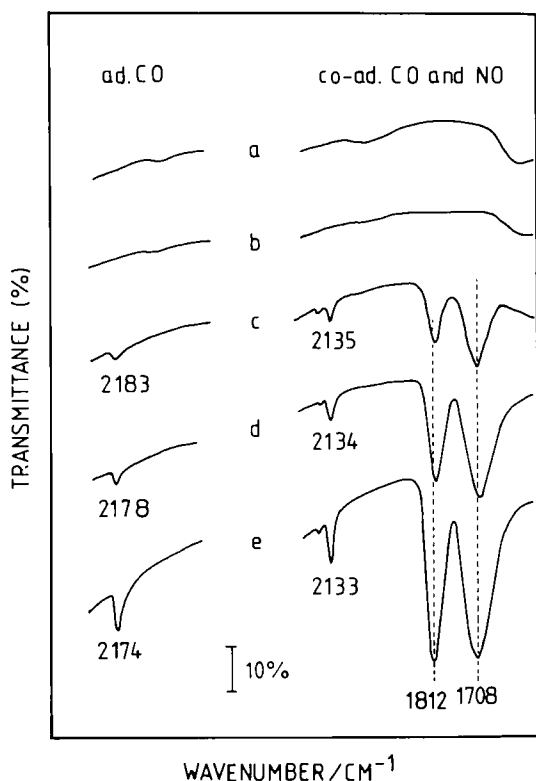


FIG. 1. Infrared spectra of adsorbed CO and coadsorbed CO-NO on 10% MO/AL₂O₃ reduced at (a) room temperature, (b) 473 K, (c) 573 K, (d) 673 K, and (e) 773 K.

frequency part of 1823 and 1731 cm⁻¹. Meanwhile two weak NO bands appear at the lower frequency part of ~1800 and ~1690 cm⁻¹, as can be seen from the difference spectrum in Fig. 2g. This phenomenon suggests that some of the NO bands at the higher frequency are associated with the CO band at 2134 cm⁻¹, and the appearance of NO bands at the lower frequency might be due to the removal of coadsorbed CO band.

The above IR results could be explained by several types of cus Mo sites. It has been reported that alumina supported molybdena catalysts reduced below 873 K contain mainly Mo⁴⁺ together with smaller amounts of Mo⁵⁺ balanced by some lower valence state (12). The cus Mo⁵⁺ sites are revealed by the CO band at ~2200 cm⁻¹. This band is unaffected by the coadsorption of NO, indicative of the absence of interaction between Mo⁵⁺ sites and NO. This is in agreement with the EPR results in a previous publication (3). Hence, the cus Mo⁵⁺ cations possess most likely 5-coordinate, denoted as Mo_{5C}⁵⁺, with only one open position exposed. For the formation of dinitrosyl species, the coordinative unsaturation of Mo cations must be higher, sufficient to permit at least two NO to adsorb at the same time. It would be further necessary to assume that one type could adsorb CO while both types adsorb NO.

The Raman spectra of 10% Mo/Al₂O₃ reduced at different temperatures are presented in Fig. 3. For the dehydrated oxidic sample, the 1000- and ~300-cm⁻¹ bands have been assigned to the monooxo molybdenum oxide species, and the band at ~210 cm⁻¹ to the polymeric molybdenum oxide species (9). The broad band observed at ~866 cm⁻¹ is due to microcrystalline molybdates formed from cationic impurities (13). When reduced at 400 K, the bands at ~210 and possibly ~940 cm⁻¹ due to the polymolybdate species disappear. Reduction at 500 K does not result in appreciable spectral change. However, after reduction at 600 K, the 1000-cm⁻¹ band decreases considerably, while a new band at ~280 cm⁻¹ and a weak shoulder at ~748 cm⁻¹ appear. Further reduction at 700 K drastically decreases the band at ~850 cm⁻¹, indicating that the reducibility of microcrystalline molybdates is the lowest among the three surface Mo species. The 280-cm⁻¹ band is now predominant in the spectrum, and the broad band at 748 cm⁻¹ can be clearly identified. The spectrum recorded after reoxidation of the reduced sample in O₂ at 700 K for 1 h is identical to that of the

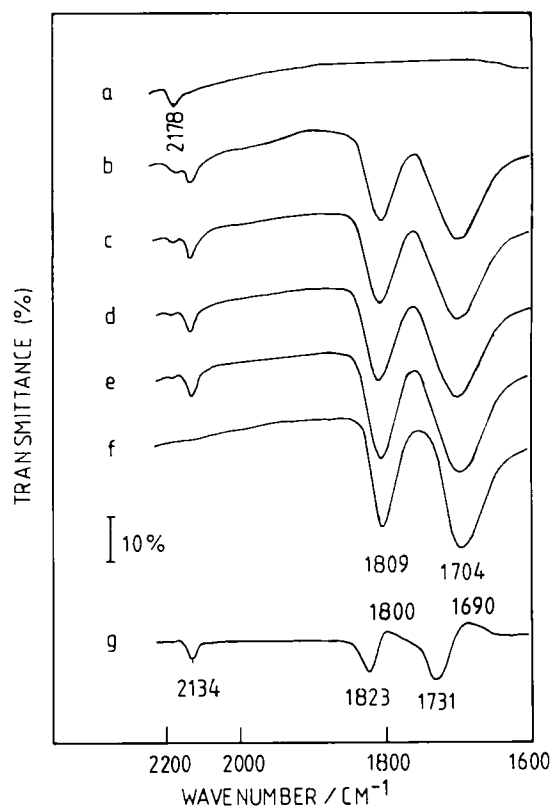


FIG. 2. Infrared spectra of preadsorbed CO on 10% Mo/Al₂O₃ (R = 673 K) as a function of NO coadsorption time. (a) Preadsorbed CO; (b) coad. NO, 5 min; (c) coad. NO, 15 min; (d) coad. NO, 45 min; (e) coad. NO, 2h; (f) 1 min evacuation after obtaining spectrum (e); and (g) difference between spectrum (e) and spectrum (f).

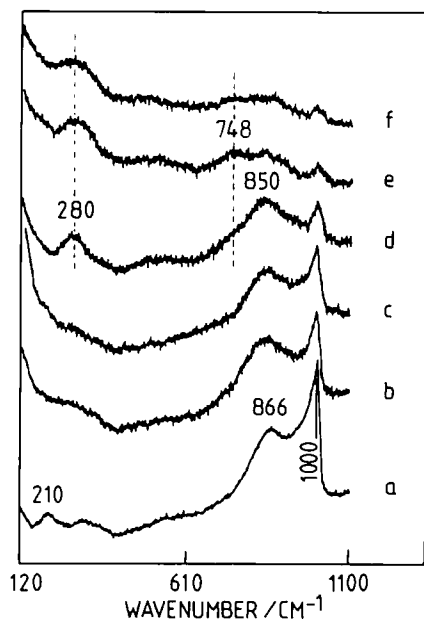


FIG. 3. Raman spectra of 10% Mo/Al₂O₃ reduced at (a) room temperature, (b) 400 K, (c) 500 K, (d) 600 K, (e) 700 K, and (f) 800 K.

freshly calcined sample shown in Fig. 3a, indicating that the reduction/reoxidation process is reversible.

After reduction at 400 K, the absence of weak bands due to the polymeric molybdenum oxide species indicates that this species can be easily reduced by H₂. However, no appreciable CO or NO adsorption band was observed, showing that the number of cus Mo sites must be very few or nonexistent at this low reduction temperature. Since the regeneration of surface hydroxyl groups has been observed to occur after reduction or sulfiding (14), it is suspected that this reduction may be associated with the reduction only of the terminal Mo=O bonds and the formation of hydroxyl groups with both the support and the dispersed molybdena, in a way somewhat similar to that reduction behavior of the supported vanadia (15). The fact that the cus Mo⁵⁺ sites for CO adsorption are so few is possibly due to the presence of hydroxyl groups with Mo⁵⁺ cations.

The two new Raman bands at ~280 and ~748 cm⁻¹ observed after reduction at 600 K and above is apparently related to the cus Mo sites which could adsorb CO and NO. The reduced Mo species cannot be crystalline MoO₂, because MoO₂ possesses quite different Raman bands at 135, 206, and 708 cm⁻¹ (16). The significant decrease of the 1000-cm⁻¹ band due to the symmetric vibration of terminal Mo=O bond suggests some correlation between the monooxo molybdenum oxide species and the reduced species. As for the initial monooxo molybdenum oxide species, its structure has been speculated as one Mo=O bond with length of 1.681 Å and four Mo-O bonds bridged

to the first oxide layer of alumina at ~1.89 Å and an opposing oxygen to the second oxide layer at more than 2.6 Å (13). Because of the ionic character, these bridging Mo⁶⁺-O bonds are Raman inactive. However, the covalence of bridging Mo-O bonds with Mo valence state lower than +6 may be higher, resulting in the observable Raman bands after reduction.

According to the formula discussed by Hardcastle and Wachs (13), the reduced Mo species with Raman bands at 280 and 748 cm⁻¹ were calculated for two Mo-O bonds with lengths of 1.825 and 2.299 Å. It is interesting to note that these two values are very similar to the two bridging Mo⁶⁺-O bond lengths proposed previously (13). The possible structures are supposed in Table 1. Three types of Mo cations are proposed to be present on the reduced 10% Mo/Al₂O₃ surface, i.e., Mo⁵⁺, Mo⁴⁺, and Mo³⁺ in 5-, 4-, and 3-coordinates, respectively. A small discrepancy exists between the calculated value and the real oxidation state. This may be due to the selection of Raman frequency used for the calculation. The broadness of the Raman bands of the reduced Mo species suggests a possible distribution of different oxidation states. For the reduced polymolybdate and microcrystalline molybdate species, it is speculated that similar Mo cations may also form, possibly with some differences in the local environment of Mo cations.

After H₂ reduction, the surface Mo species have been reported to rearrange and agglomerate to create some free alumina which is a function of the extent of reduction (17). Some Mo-O-Al bridging bonds are broken on reduction, which results in the formation of Mo cations with different coordination unsaturation. From the proposed surface structures of the reduced Mo species in Table 1, the infra-

TABLE 1
Possible Molecular Structures of Surface Molybdenum Oxide Species after H₂ Reduction

	O Mo ⋮ O	Mo / \ / \ O O O O ⋮ O	Mo / \ / \ O O O O ⋮ O	Mo / \ / \ O O O O ⋮ O
First oxygen layer of alumina	O	O	O	O
Second oxygen layer of alumina	O	O	O	O
Calculated valence state		5.11	3.92	2.73
Real oxidation state	6	5	4	3
Coordination number	6	5	4	3

red spectroscopy of CO and NO adsorptions could be interpreted. $\text{Mo}_{3\text{C}}^{5+}$ site coordinates one CO molecule, because there is just one open position exposed. For $\text{Mo}_{4\text{C}}^{4+}$ site with two open positions exposed, both CO and NO can adsorb as a dimer. The $\text{Mo}^{4+}(\text{CO})_2$ has been observed by some authors (2, 6), however, its stability was found to be very low. On the contrary, $\text{Mo}_{4\text{C}}^{4+}(\text{NO})_2$ seems to be very stable. The adsorption of CO on $\text{Mo}_{3\text{C}}^{3+}$ site which possesses three open positions exposed, forms a tetrahedral complex. This complex can further accommodate another two NO molecules to form an octahedral complex. Without coadsorbed CO, due to the higher electron density on $\text{Mo}_{3\text{C}}^{3+}$ site, $\text{Mo}_{3\text{C}}^{3+}(\text{NO})_2$ should exhibit a lower IR stretching frequency as compared to $\text{Mo}_{4\text{C}}^{4+}(\text{NO})_2$, as evidenced by the IR results presented above. Hall and his co-workers (18) have reported that small amounts of CO or NO were effective poisons for hydrogenation and isotope exchange. That can only be accounted for by the poisoning of $\text{Mo}_{3\text{C}}^{3+}$ cation sites. In conclusion, three types of cus Mo sites are present together on the reduced 10% Mo/ Al_2O_3 after reduction at 573 K and above, and their relative amounts appear in the order: $\text{Mo}^{4+} \gg \text{Mo}^{3+} > \text{Mo}^{5+}$.

The previous assignments for IR frequency of adsorbed CO in the region 2194–2172 cm^{-1} are quite conflicting. Both $\text{Mo}^{3+}(\text{CO})$ and $\text{Mo}^{4+}(\text{CO})$ have been suggested. Due to the similarity of these CO bands, it is difficult to distinguish the different cus Mo sites. Moreover, the influence from the coexisted CO band due to adsorption on Mo^{5+} sites makes these assignments questionable. The IR spectra of coadsorbed CO–NO clearly show that only two CO bands at ~ 2200 and 2134 cm^{-1} are present and their frequencies do not change noticeably with the change of extent of reduction, suggesting that only two types of cus Mo sites are responsible for the CO adsorption. The most possible sites are $\text{Mo}_{3\text{C}}^{5+}$ and $\text{Mo}_{3\text{C}}^{3+}$ cations. It is argued that the downward shift of CO band from 2183 to 2174 cm^{-1} with increasing extent of reduction might be due to the decreased component of adsorbed CO on $\text{Mo}_{3\text{C}}^{5+}$ sites. However, due to the oxidizing charac-

ter of NO (12), the presence of very small amount of cus Mo cations with valence state lower than +3 before NO adsorption cannot be excluded.

REFERENCES

1. Peri, J. B., *J. Phys. Chem.* **86**, 1615 (1982).
2. Zaki, M. L., Vielhaber, B., and Knözinger, H., *J. Phys. Chem.* **90**, 3176 (1986).
3. Valyon, J., and Hall, W. K., *J. Catal.* **84**, 216 (1983).
4. Yan, Y., Xin, Q., Jiang, S., and Guo, X. X., *J. Catal.* **131**, 234 (1991).
5. Delgado, E., Fuentes, G. A., Hermann, C., Kunzmann, G., and Knözinger, H., *Bull. Soc. Chim. Belg.* **83**, 735 (1984).
6. Peri, J. B., in "Catalysis—Science and Technology" (J. R. Anderson and M. Boudart, Eds.), Vol. 5, p. 171. Springer-Verlag, Berlin, 1984.
7. Guglielminotti, E., and Giamello, E., *J. Chem. Soc. Faraday. Trans. 1* **81**, 2307 (1985).
8. Kim, D. S., Segawa, K., Soeya, T., and Wachs, I. E., *J. Catal.* **136**, 539 (1992).
9. Vuurman, M. A., and Wachs, I. E., *J. Phys. Chem.* **96**, 1008 (1992).
10. Segawa, K., and Millman, W. S., *J. Catal.* **101**, 218 (1986).
11. Sheppard, W., and Nguyen, T. T., *Adv. Infrared Raman Spectrosc.* **5**, 67 (1978).
12. Redey, A., Goldwasser, J., and Hall, W. K., *J. Catal.* **113**, 82 (1988).
13. Hardcastle, F. D., and Wachs, I. E., *J. Raman Spectrosc.* **21**, 623 (1990).
14. Millman, W. S., Segawa, K., Serz, D., and Hall, W. K., *Polyhedron* **5**, 169 (1986).
15. Went, G. T., Leu, L., and Ell, A. T., *J. Catal.* **134**, 479 (1992).
16. Schrader, G. L., and Cheng, C. P., *J. Catal.* **80**, 369 (1983).
17. O'Young, C. L., Yang, C. H., DeCanio, S. J., Patel, M. S., and Storm, D. A., *J. Catal.* **113**, 307 (1988).
18. Lombardo, E. A., Lo Jacono, M., and Hall, W. K., *J. Catal.* **64**, 150 (1980).

Xingtao Gao
Qin Xin

State Key Laboratory of Catalysis
Dalian Institute of Physical Chemistry
Chinese Academy of Sciences
Dalian 116023
People's Republic of China

Received May 12, 1993; revised September 20, 1993